Photoinduced Selective B–H Activation of *nido*-Carboranes

Shengwen Xu[1], Hongjian Zhang[1], Jingkai Xu[1], Weiqun Suo[2], Chang-sheng Lu[1], Deshuang Tu[1]*, Xingwei Guo[2]*, Jordi Poater[3,4]*, Miquel Solà[5]*, and Hong Yan[1]*

[1]State Key Laboratory of Coordination Chemistry, Jiangsu Key Laboratory of Advanced Organic Materials, School of Chemistry and Chemical Engineering, Nanjing University, Nanjing 210023, China

[2]Center of Basic Molecular Science, Department of Chemistry, Tsinghua University, Beijing 100084, China

[3]Departament de Química Inorgànica i Orgànica & IQTCUB, Universitat de Barcelona, Martí i Franquès 1-11, Barcelona 08028, Spain

[4]ICREA, Pg. Lluís Companys 23, Barcelona 08010, Spain

[5]Institut de Química Computacional i Catàlisi and Departament de Química, Universitat de Girona, C/ Maria Aurèlia Capmany 69, Girona 17003, Catalonia, Spain

ABSTRACT: The development of new synthetic methods for B–H bond activation has been an important research area in boron cluster chemistry, which may provide opportunities to broaden the application scopes of boron clusters. Herein, we present a new reaction strategy for the direct site-selective B–H functionalization of *nido*-carboranes initiated by photoinduced cage activation via a non-covalent cage···π interaction. As a result, the *nido*-carborane cage radical is generated through a single electron transfer from the 3D *nido*-carborane cage to the 2D photocatalyst upon irradiation of green light. The resulting transient *nido*-carborane cage radical could be directly probed by an advanced time-resolved EPR technique. In air, the subsequent transformations of the active *nido*-carborane cage radical have led to efficient and selective B–N, B–S, and B–Se couplings in the presence of N-heterocycles, imines, thioethers, thioamides, and selenium ethers. This protocol also facilitates both the late-stage modification of drugs and the synthesis of *nido*-carborane-based drug candidates for boron neutron capture therapy (BNCT).

INTRODUCTION

The development of a novel reaction mode is a central topic in synthetic chemistry as it enables the realization of previously unattainable chemical transformations, complements or even supplants conventional synthetic routes, and facilitates access to highly complex and valuable molecular architectures. In comparison to the diverse methods for functionalization of organoboron molecules,[1,2] the direct functionalization of boron clusters lags far behind and represents considerable challenges due to the unique molecular compositions and structures of these clusters.

Boron clusters, such as *closo*- and *nido*-carboranes, are three-dimensional (3D) aromatic species with spherical molecular geometry and multiple-center, multiple-electron bonding structures.[3,4] Owing to the wide range of applications in different fields,[5] the functionalization of boron clusters has garnered tremendous research interest.[6−12] However, these boron clusters possess more than several B–H bonds in a similar chemical environment with a high bond dissociation energy that is comparable to those of the C(sp^3)–H bonds.[13] These factors collectively complicate the selective B–H functionalization of boron clusters with organic functionalities. In this study, we focused on *nido*-carboranes, the open-cage analogues of *closo*-carboranes. The different synthetic strategies such as nucleophilic substitution,[9] electrophilic substitution,[10] oxidative substitution,[11] and metal mediation (Figure 1a),[12] have been developed for the B–H functionalization of *nido*-carboranes. However, these reaction protocols frequently require the use of metal complex, ligand, oxidant, even an elevated temperature to access structurally specified *nido*-carborane derivatives. Undoubtedly, the development of practical, versatile, and modular approaches to functionalize *nido*-carboranes is highly desirable, yet remains a synthetic challenge.

Recently, our group discovered a new type of non-covalent bond, denoted as a cage···π interaction,[14] which is formed from the interaction between 3D *nido*-carborane and a two-dimensional (2D) π unit. The cage···π interaction enables promoting the facile charge transfer (CT) from the 3D *nido*-carborane cage to the 2D aromatic ring, similar to those occurred in the conventional electron donor-acceptor (EDA) complexes.[15] This inspired us to explore the possible applications of such a non-covalent cage···π interaction in new synthetic methods.

In this study, to address the challenge in the B–H functionalization of *nido*-carboranes, we used the non-covalent cage···π interaction to develop a new strategy for realization of the efficient and direct B–H functionalization

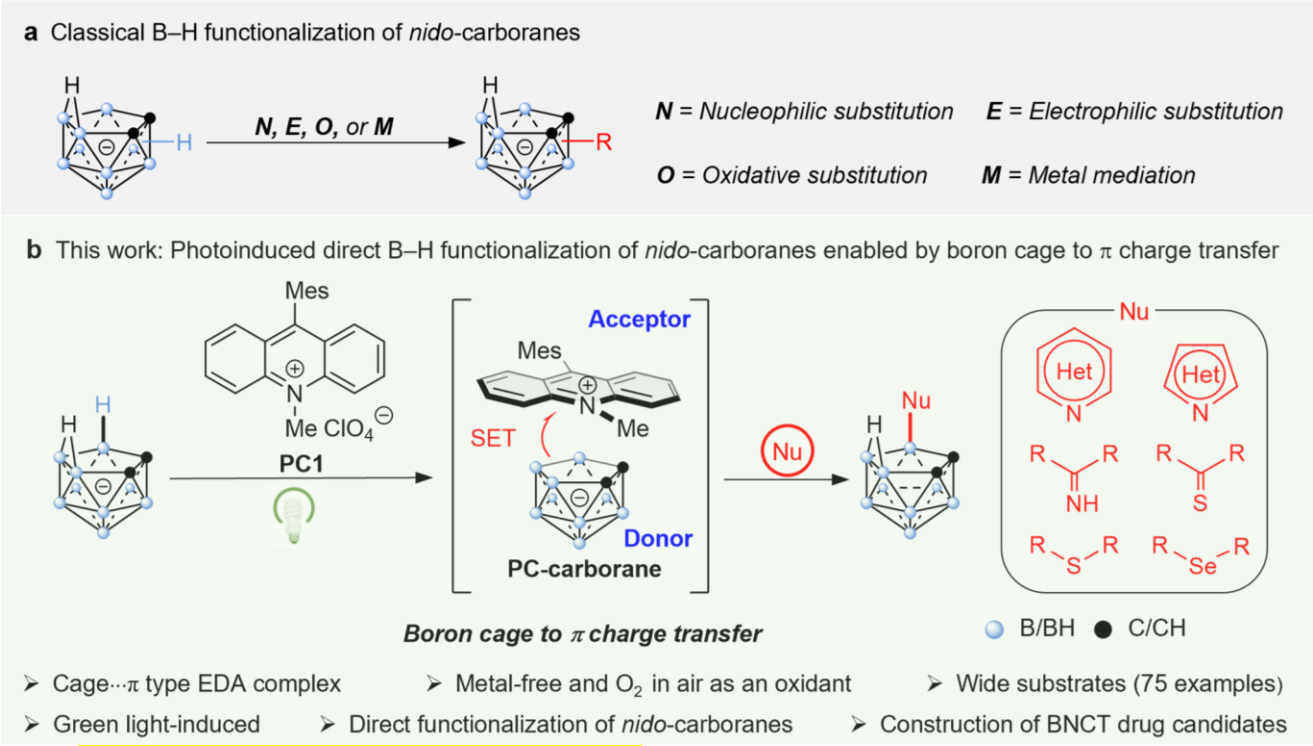

Figure 1 (a) Classical B–H functionalization of *nido*-carboranes. (b) This work: Photoinduced direct B–H functionalization of *nido*-carboranes via a SET process through a novel non-covalent cage···π type EDA complex (**PC-carborane**). The B–H–B bridging hydrogen in **PC-carborane** is omitted for clarity.

of *nido*-carboranes (Figure 1b). In doing so, we chose the widely used the 2D aromatic photocatalyst acridinium perchlorate[16] in order to create a cage···π type EDA complex (**PC-carborane**, Figure 1b) with the 3D aromatic *nido*-carborane anion. The generation of such a cage···π type EDA complex has been experimentally verified by X-ray crystallography in the solid state and spectral techniques in solution (Figures 2 and 3). Under the irradiation of green light, a single electron transfer (SET) process from the boron cage to the acridine ring could take place. The resulting *nido*-carborane cage radical could be oxidized by O_2 in air through a unusual bridging B–H–B hydride transfer (HAT) to generate a highly electrophilic *nido*-carborane cage, which then reacts with differing nucleophilic substrates such as N-heterocycles, imines, thioethers, thioamides, and selenium ethers to construct versatile carborane derivatives containing a B–X (X = N, S, Se) bond. Note that for the first time the in situ generated transient *nido*-carborane cage radical has been successfully detected and characterized by an advanced time-resolved EPR technique. The reaction protocol proceeds in a metal-free and photocatalytic manner in air with a green light at room temperature to give rise to a yield of up to 99%. Moreover, the synthetic applications also have been demonstrated in several complex settings such as one-step late-stage modification of drugs and the synthesis of drug candidates for boron neutron capture therapy (BNCT).

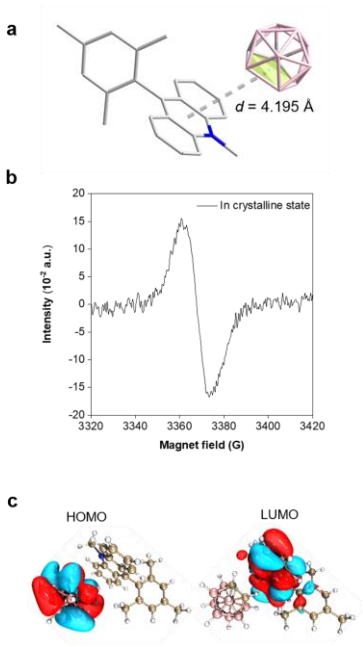

Figure 2. (a) The single-crystal structure of **PC-carborane** EDA complex. The hydrogen atoms are omitted for clarity. (b) The electron paramagnetic resonance (EPR) spectrum of **PC-carborane** EDA complex in the crystalline state under light irradiation. (c) HOMO and LUMO of **PC-carborane** EDA complex in the excited state.

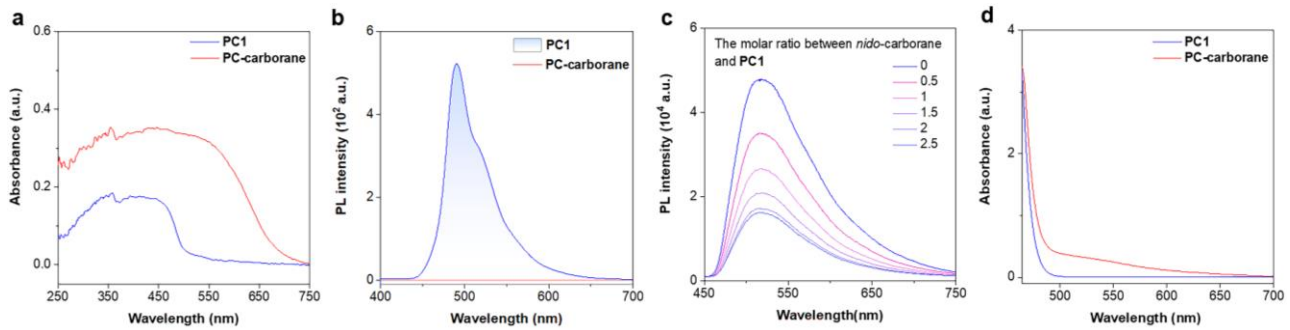

Figure 3. (a) UV/Vis absorption spectra in the crystalline state for **PC1** and **PC-carborane**. (b) PL spectra of **PC1** and **PC-carborane** in the crystalline state. (c) PL spectra of **PC1** in the presence of different molar ratios of *nido*-carborane anion in DCM (c = 10.0 μM). (d) UV/Vis absorption spectra of **PC1** and **PC-carborane** in DCM (c = 1.0 mM).

RESULTS AND DISCUSSION

Design of the reaction system. In recent years, photoredox catalysis has emerged as a powerful tool for the development of selective functional group-specific coupling protocols through the generation of open-shell radical intermediates.[17] We have explored the photocatalytic reactions for the B–H functionalization of carboranes.[8c,18] For example, the synthetic strategies through decarboxylation coupling[8c] and hydrogen atom transfer[18] have been developed to generate highly active boron-center carborane radicals, which further react to lead to the B–H functionalization. In this study, we still used a photoinduced fashion but introduced a new type of non-covalent cage···π interaction to develop an innovative reaction mode aiming to achieve the straightforward and site-selective B–H functionalization of *nido*-carboranes. Thus 9-mesityl-10-methylacridinium perchlorate (Mes-AcrClO$_4$, **PC1**), an extensively utilized photocatalyst,[16] was chosen as it contains an electron-deficient aromatic acridinium unit, which may meet the requirement to establish a cage···π interaction[14] with an aromatic *nido*-carborane cage anion.

Indeed, when mixing *nido*-carborane and **PC1**, we obtained the expected cage···π type EDA complex in crystalline state as shown in Figure 2a by a single crystal structure analysis, denoted as **PC-carborane** EDA complex (Figure 1b). The EPR measurement on the crystalline sample showed a clear signal under light irradiation (Figure 2b), demonstrating the facile SET process from the *nido*-carborane cage to acridinium. The theoretical calculations on electronic distributions in the **PC-carborane** EDA complex in the excited state further support the charge transfer from the boron cage to the π ring (Figure 2c). Furthermore, a large red-shift (~ 110 nm) in UV/Vis absorption spectra (Figure 3a) and emission quenching (Figure 3b) in PL spectra were observed for the **PC-carborane** EDA complex in comparison to **PC1** in the crystalline state. Both are attributed to the charge transfer in the EDA complex generated by the cage···π interaction. These phenomena also appeared in other EDA complexes.[15] How does the cage···π type EDA complex behave in solution? By titration

Table 1. Reaction development

1-1 2-1 3-1

Entry	Variation from conditions	Yield (%)[b]
1[a]	None	92
2	**PC2** instead of **PC1**	8
3	**PC3** instead of **PC1**	21
4	THF instead of DCM	71
5	$CHCl_3$ instead of DCM	47
6	Acetone instead of DCM	63
7	KPF_6 instead of NH_4PF_6	58
8	NH_4F instead of NH_4PF_6	37
9	Without **PC1**	No
10	Without light	No
11	Ar instead of air	No

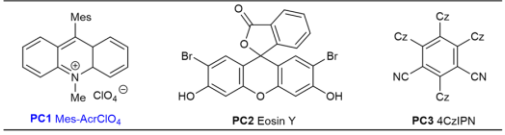

(a) **1-1** (0.1 mmol), pyridine (**2-1**, 0.2 mmol), NH_4PF_6 (0.1 mmol), photocatalyst (5 mol%), DCM (2.0 mL), 3 W green LEDs, air, room temperature, 3 h, as the standard conditions. (b) Isolated yields of **3-1**. Mes = mesitylene, Cz = carbazole.

of *nido*-carborane, the PL spectra of **PC1** showed decreasing emission intensity (Figure 3c), reflecting the charge transfer between the *nido*-carborane anion and acridinium. In addition, the UV/Vis absorption spectra also demonstrated an obvious red shift to the green light absorption region in contrast to **PC1** (Figure 3d) owing to the charge transfer in the EDA complex. Thereby the photoinduced functionalization of *nido*-carborane may take place via such an EDA complex under green light.

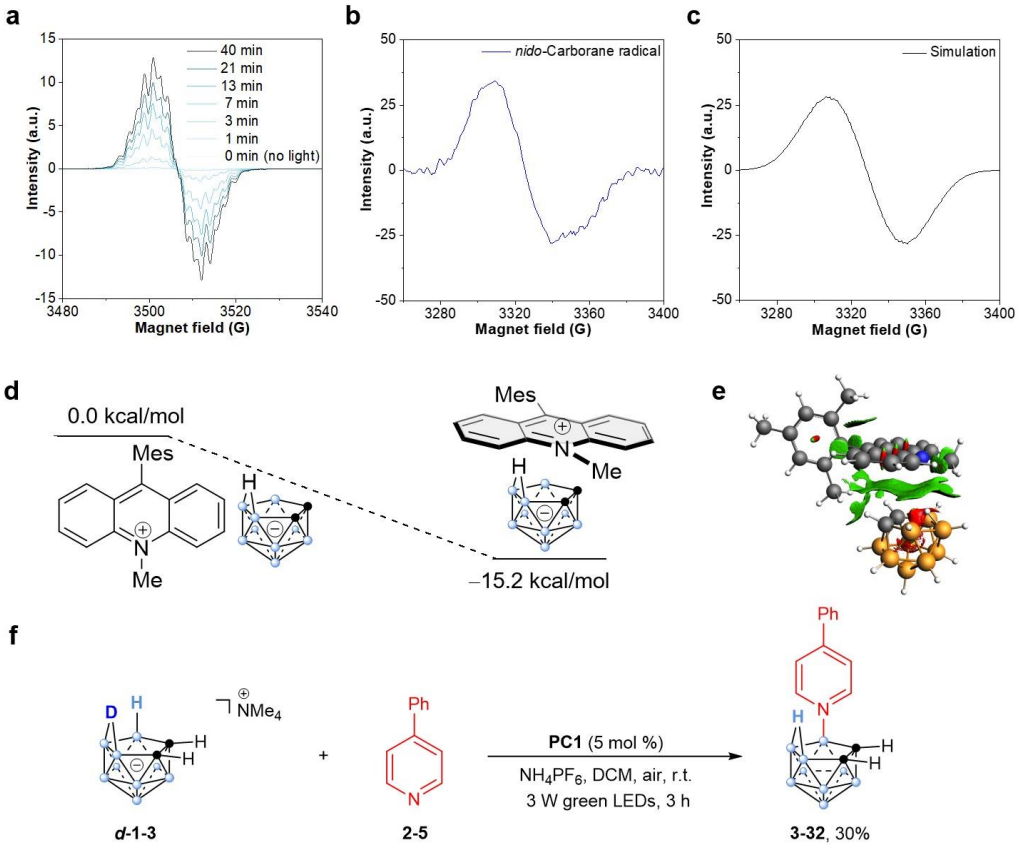

Figure 4. (a) The in situ steady-state EPR spectra of acridine radicals in the tracking experiments (MW freq. = 9.82 GHz). (b) The transient EPR signal of the *nido*-carborane cage radical in solution measured by an advanced time-resolved EPR technique (MW freq. = 9.33 GHz). (c) The simulated EPR signal of the *nido*-carborane cage radical. (d) The theoretical calculations of **PC-carborane** EDA complex in solution. (e) The non-covalent interaction (NCI) plot of **PC-carborane** EDA complex. (f) Deuterium labeling experiment.

Reaction development. Based on the above understanding of the new EDA complex (**PC-carborane**) both in the solid state and in solution, we examined the feasibility of a photocatalytic strategy for the B–H functionalization of *nido*-carborane by nucleophilic reagents. Firstly, (NMe_4)(7,8-Ph_2-*nido*-$C_2B_9H_{10}$) **1-1** and pyridine **2-1** were chosen as the model substrates (Table 1). By screening different photocatalysts, solvents, and additives, we obtained the best reaction conditions. Under the irradiation of 3 W green LEDs, the reaction of *nido*-carborane with pyridine in the presence of 5 mol% **PC1** and NH_4PF_6 in CH_2Cl_2 in air at room temperature for 3 h afforded the product **3-1** in an isolated yield of 92% (entry 1). Note that according to the literature,[16c] a SET process did not occur by using **PC1** as a photocatalyst under green light as its absorption band is located in the UV and blue light regions (Figure S5b). However, here the UV/Vis spectrum of **PC-carborane** in solution presents new absorption in the green light region (Figure 3d). Thus, the reaction could take place under green light but via the **PC-carborane** EDA complex. Other photocatalysts including Eosin Y (**PC2**) and 4CzIPN (**PC3**) were much less reactive (entries 2 and 3). In addition, the solvents such as THF, $CHCl_3$, and acetone led to lower yields (entries 4 to 6). Different additives instead of NH_4PF_6 were also used (entries 7 and 8), but lower reaction yields were observed. No reaction occurred without photocatalyst or light, or instead of air by argon (entries 9 to 11).

Mechanistic studies. Having the established optimal reaction conditions, we proceeded to undertake a series of experiments aimed at gaining a profound understanding on the reaction mechanism. Firstly, we set up the following experiments to investigate reaction intermediates. If pyridine was not added, only **PC-carborane** was isolated in a 90% yield (Figure S6). However, the subsequent addition of pyridine to the above reaction system led to the formation of the B–N coupling product, demonstrating that **PC-carborane** could be the intermediate (Figure S6). Then, the addition of 2,2,6,6-tetramethylpiperidine-1-oxyl (TEMPO) to the reaction system led to the trace product (Figure S7), suggesting a radical-involved process. However, we could not capture the species generated by the *nido*-carborane radical with the TEMPO radical coupling or with 1,1-diphenylethylene addition (Figure S7), demonstrating a delocalized *nido*-carborane radical. Theoretical calculations support that the unpaired electron is distributed throughout the boron cage rather than being localized on a single boron atom (Figures S8 and S9).

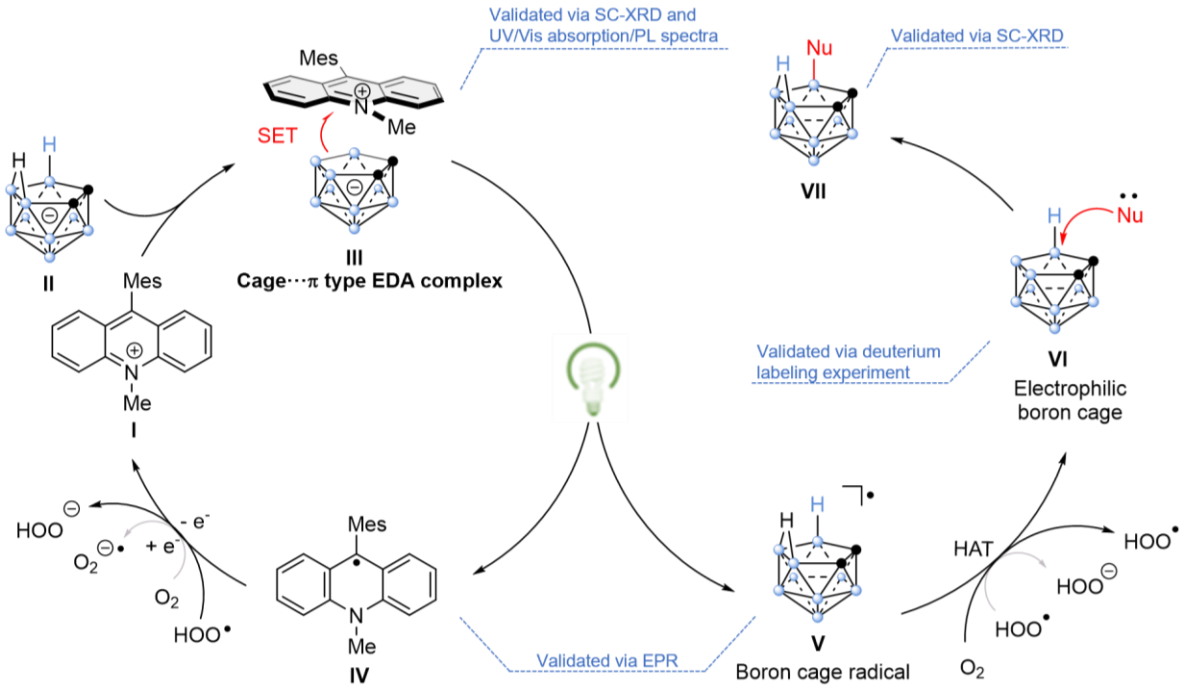

Figure 5. Proposed reaction mechanism. The B–H–B bridging hydrogen atom in the **PC-carborane** EAD complex is omitted for clarity.

Next, the in-situ steady-state EPR technique was utilized to detect the radical intermediates involved in the reaction system. As a result, the acridine radical was readily captured and identified by its characteristic anisotropic signal with g = 2.0027 (Figure 4a) in comparison with the literature report.[16e] However, the *nido*-carborane radical could not be observed in the reaction system, which may be attributed to its short lifetime or quick subsequent conversion. Recently, one of the authors' team has developed an advanced time-resolved EPR technique based on innovative ultrawide single sideband phase-sensitive detection (U-PSD), namely U-PSD TREPR, which provides exceptional detection sensitivity for radical intermediates in the course of reaction.[19] This technique enabled us to directly probe the transient *nido*-carborane radical in this study. To our delight, a transient EPR spectrum centered at g = 2.0047 was successfully acquired by integrating 0-5 μs after the laser pulse (Figure 4b), which exhibited a broad signal (peak to peak linewidth 30G), consistent with a delocalized boron cage radical.[20] This is further supported by the spectrum simulation obtained by DFT calculations (Figure 4c). The short lifetime observed for this radical species (~ 2.5 μs, Figure S12c) demonstrated the transient and active nature of the *nido*-carborane radical intermediate. To the best of our knowledge, this is the first EPR spectrum reported on the *nido*-carborane cage radical. In contrast, other stable *closo*-boron cage radicals have been well investigated.[20]

On the other hand, the theoretical calculations at the ZORA-BLYP-D3(BJ)/TZ2P level also demonstrate the formation of the **PC-carborane** EDA complex is energetically favorable in solution (Figures 4d, S13 and Table S2) on the basis of the cage···π interaction where the electrostatic interaction between the whole *nido*-carborane anion and the cationic photocatalyst predominates (Table S1). This is further proven by a non-covalent interaction (NCI) plot (Figure 4e).

Furthermore, a deuterium labeling experiment was performed by using the deuterated *nido*-carborane containing a bridging B–D–B bond. As a result, product **3-32** was isolated, rather than deuterated **3-32** (Figures 4f and S14). Therefore, we deduced that the bridging deuterium is firstly oxidized by air as it is more reductive and then replaced by the terminal B(9)–H.[21] Such a process is driven by the subsequent nucleophilic attack from pyridine. Here the reduced yield (30% vs 70%) of **3-32** should be attributed to the isotope effect.

Based on above results, we proposed a mechanism as outlined in Figure 5. Firstly, the EDA complex (**III**) is formed between the acridine cation (**I**) and the *nido*-carborane anion (**II**). Under the green light irradiation, a SET process takes place in the EDA complex (**III**) to generate the acridine radical (**IV**) and the *nido*-carborane cage radical (**V**). In the presence of oxygen in air or hydroperoxy radical, the *nido*-carborane radical (**V**) undergoes hydrogen atom transfer (i.e. the bridging hydride involved HAT), which leads to an active electrophilic boron cage (**VI**). The subsequent reaction of intermediate (**VI**) with a nucleophilic reagent gives rise to the functionalized carborane (**VII**) at the B(9) site where is more electron-deficient. The acridine radical (**IV**) can be oxidized by oxygen in air or hydroperoxy radical to regenerate the ground-state acridine cation (**I**), thus completing the catalytic cycle.[16b]

Scheme 1. Substrate Scope for B–N Cross-Coupling.

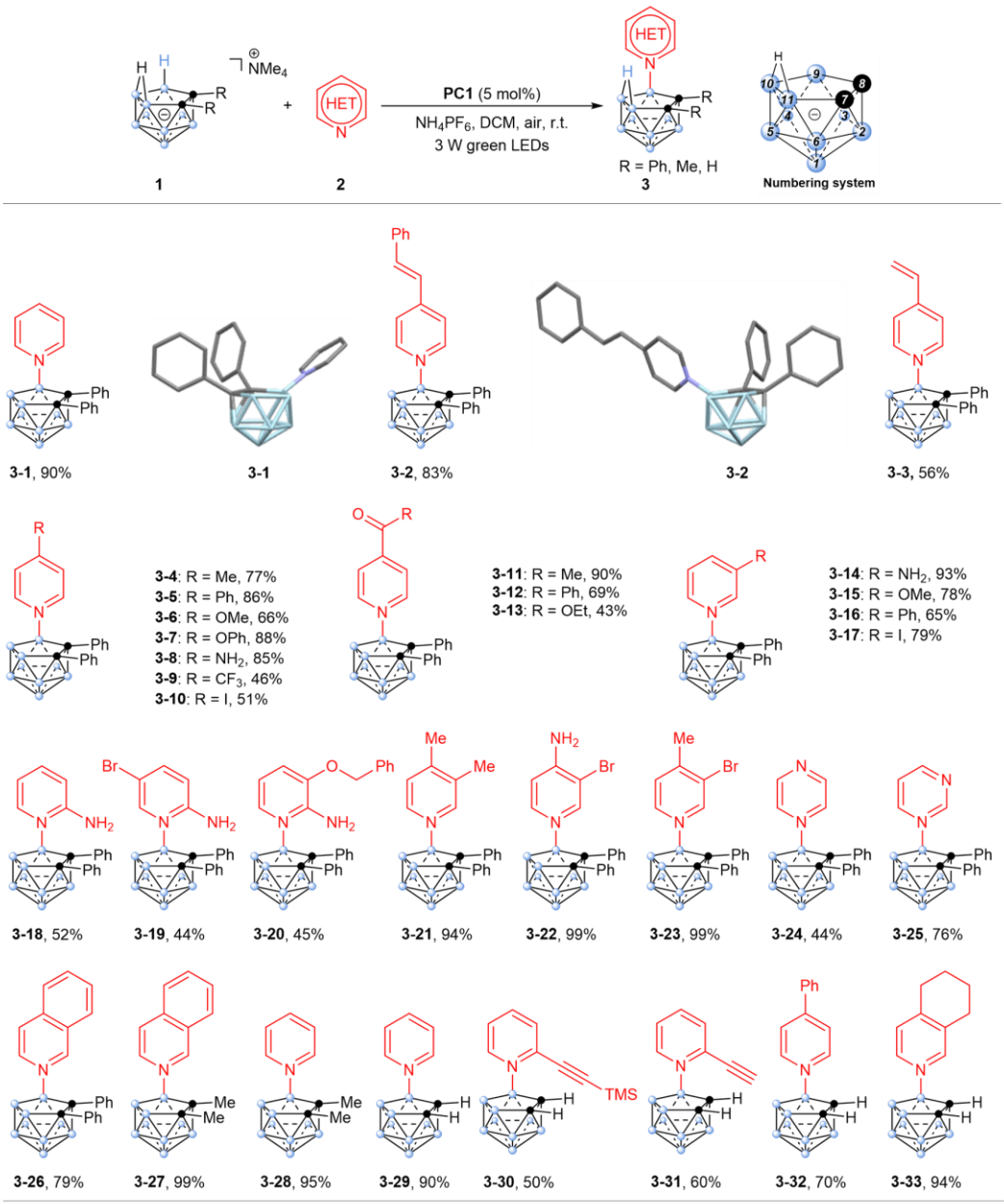

Reaction scope I. **1** (0.1 mmol), **2** (0.2 mmol), NH_4PF_6 (0.1 mmol), **PC1** (5 mol%), DCM (2.0 mL), 3 W green LEDs, air, room temperature, 3 h, as the standard conditions. The B–H–B bridging hydrogen in **3-1** to **3-33** and the hydrogen atoms in crystal structures are omitted for clarity.

Reaction Scope. On the basis of the optimized set of conditions (Table 1, entry 1) and the understanding of the reaction mechanism (Figure 5), we next evaluated the substrate scope of the green light-induced crossing coupling between *nido*-carboranes (**1-1** to **1-3**) and N-heterocycles (Scheme 1). We were pleased to find that plentiful N-heterocycles could react with *nido*-carboranes to provide B–N coupled products with good to excellent yields under standard conditions. Firstly, we began substrate expansion of pyridine compounds containing different substituents, as shown in Scheme 1. When the *para*-position of pyridines was substituted by an electron-donating group good to excellent isolated yields of the target products were obtained (**3-1** to **3-8**). However, the electron-withdrawing groups led to moderate yields (i.e. **3-9** and **3-13**) owing to the reduced nucleophilicity of the pyridine substrates. We also developed the gram-scale synthesis of **3-1** and obtained the product in an isolated yield of 67%, demonstrating the synthetic potential of this reaction protocol. In the cases of *meta*-substituted pyridines, the products could be isolated in good to excellent yields as well (**3-14** to **3-17**). If the *ortho*-position of pyridines was replaced by alkyl or aryl,

Scheme 2. Substrate Scope for B–N Cross-Coupling.

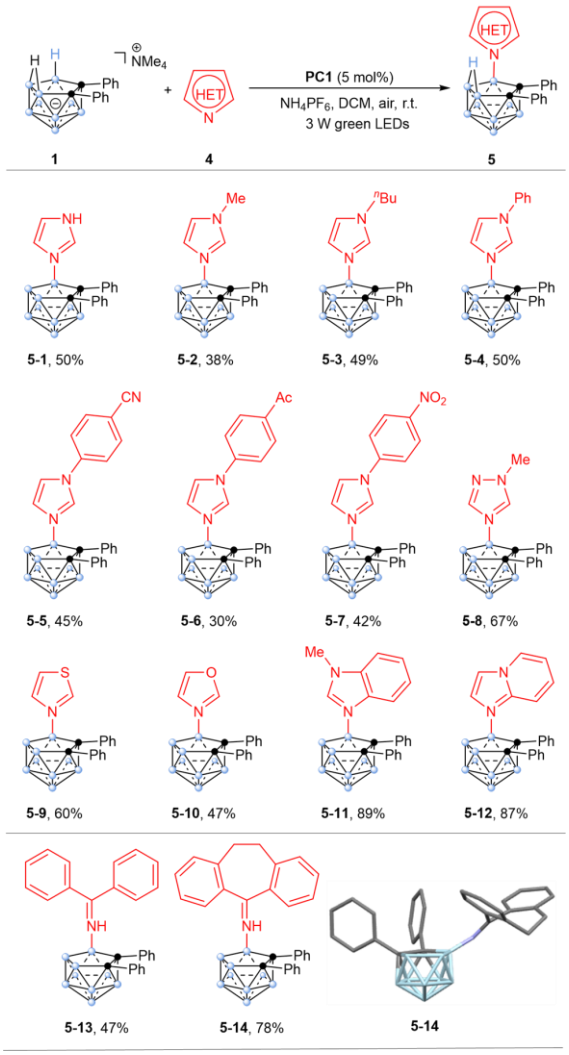

Reaction scope II. **1** (0.1 mmol), **4** (0.2 mmol), NH_4PF_6 (0.1 mmol), **PC1** (5 mol%), DCM (2.0 mL), 3 W green LEDs, air, room temperature, 3 h as the standard conditions. The B–H–B bridging hydrogen in **5-1** to **5-14** and the hydrogen atoms in crystal structures are omitted for clarity.

the yields were poor because of the large steric hindrance. If an amino group is localized at *ortho*-position, the reactions led to moderate yields (**3-18** to **3-20**). In contrast, both *para*- and *meta*-substituted pyridines afforded excellent yields (**3-21** to **3-23**). Moreover, diazacyclic compounds such as pyrazine and pyrimidine are compatible to give acceptable yields (**3-24** and **3-25**). By the change of the substituents at the carbon sites of the *nido*-carboranes, comparable outcomes were also obtained (**3-27** to **3-33**). Note that the *ortho*-substituted pyridines by alkynyl groups gave rise to moderate yields (**3-30** and **3-31**), further demonstrating the impact of steric hindrance. The polycyclic N-heterocycles such as isoquinoline and tetrahydroisoquinoline performed well to lead to excellent yields (**3-26**, **3-27**, and **3-33**).

Scheme 3. Substrate Scope for B–S Cross-Coupling.

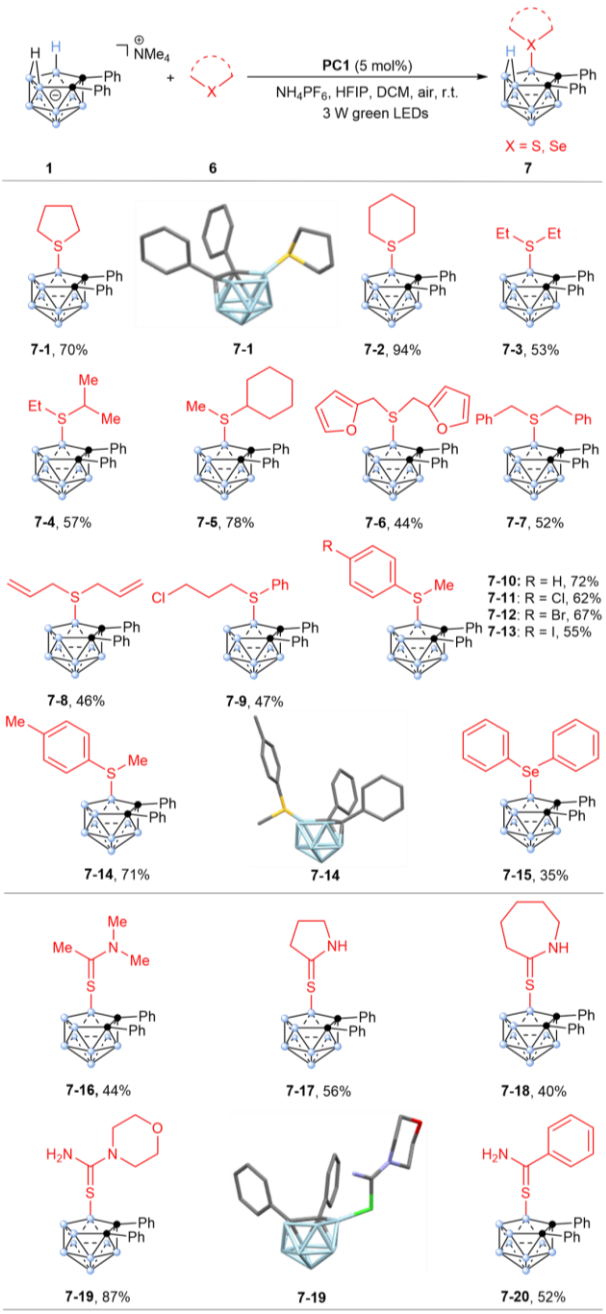

Reaction scope III. **1** (0.1 mmol), **6** (0.2 mmol), NH_4PF_6 (0.1 mmol), **PC1** (5 mol%), HFIP (0.1 mL), DCM (2.0 mL), 3 W green LEDs, air, room temperature, 12 h. The B–H–B bridging hydrogen in **7-1** to **7-20** and the hydrogen atoms in crystal structures are omitted for clarity.

Other N-heterocyclic substrates such as imidazoles were also applicable to the reaction under the standard conditions (Scheme 2). When the imidazole was substituted by an alkyl or aryl group, the target products were isolated in moderate yields (**5-1** to **5-7**). Similarly, the B–N coupling protocol was effective across diverse heterocyclic substrates. For example, 1-methyl triazole (**5-8**), thiazole (**5-9**),

Scheme 4. Synthetic applications for construction of carborane-based functionalized molecules. The B–H–B bridging hydrogen in **8-1** to **8-8** are omitted for clarity.

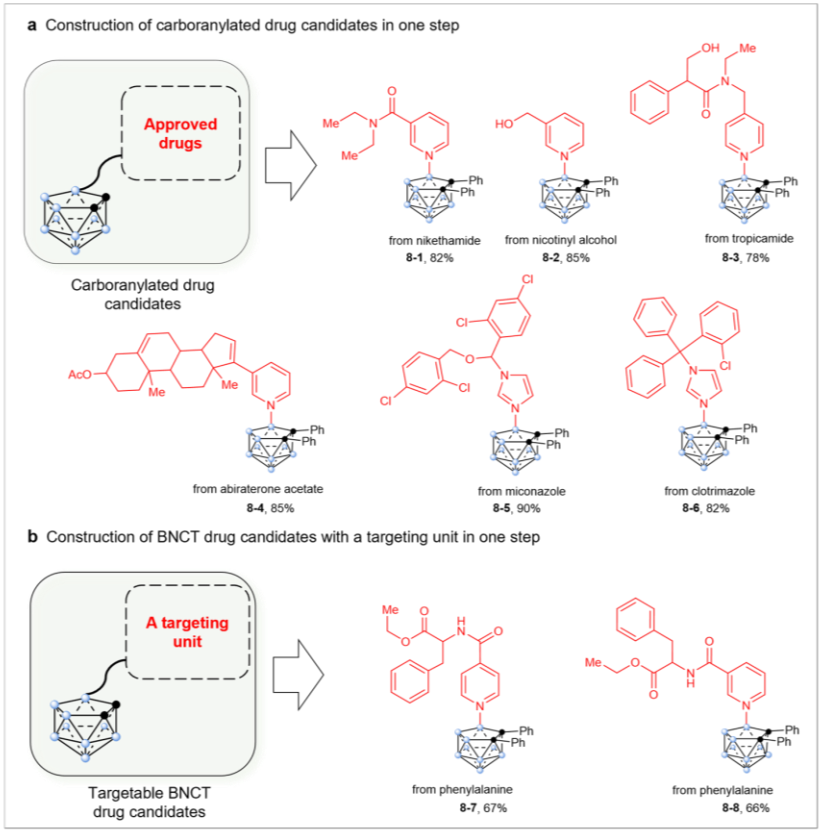

oxazole (**5-10**), 1-methyl benzimidazole (**5-11**), and imidazole [1,2-a] pyridine (**5-12**) furnished carborane-based heterocyclic products in moderate to excellent yields. Unexpectedly, the imines such as benzophenone imine and 10,11-dihydro-5H-dibenzo [a, d][7] annulene-5-imine also reacted with *nido*-carborane under standard conditions to give satisfying yields (**5-13** and **5-14**). In general, the weak nucleophilicity or electron-withdrawing group of the substrates reduces reaction yield.

Encouraged by the above B–N coupling with various N-heterocyclic substrates, we further explored the B–S coupling under the same photocatalytic system (Scheme 3). By slightly adjusting the reaction conditions using DCM and HFIP as the mixed solvents, B–S coupled products could be generated. Then, the scope of this transformation was examined. Firstly, different thioethers were tested. Good to excellent isolated yields were obtained when alkyl thioethers were used as substrates (**7-1** and **7-5**). The presence of electron-withdrawing functional groups such as furyl, phenyl, and alkenyl at the α-position of thioether resulted in decreased yields (**7-6** to **7-8**). In the cases of the mixed alkyl and aryl thioethers, the *para*-substituents in the aryl groups have less influence on the yields (**7-9** to **7-14**). However, the reaction did not work for diphenyl thioether, which should be attributed to the weakened nucleophilicity triggered by phenyl groups. However, diphenyl selenium could be coupled with *nido*-carborane owing to the stronger nucleophilicity of selenium than sulfur (**7-15**, Scheme 3). The further extension to thioamides such as dimethylthioacetamid (**7-16**), thiopyrrolidone (**7-17**), azepane-2-thione (**7-18**), 4-thiocarbamoyl-morpholine(**7-19**) and thiobenzamide (**7-20**) was also successful (Scheme 3).

The above B–N, B–S, and B–Se coupled products were carefully characterized by ^{1}H, ^{11}B, and ^{13}C NMR spectra and HRMS. The SC-XRD analysis of **3-1**, **3-2**, **5-14**, **7-1**, **7-14**, and **7-19** unambiguously confirmed the exclusive site selectivity (Schemes 1–3).

Synthetic applications. Carboranes can be a unique type of pharmacophore that binds to a protein through hydrophobic interactions, which fully takes advantage of the low-polarity nature of B–H bonds.[22] The utilization of carboranes in medicinal chemistry enables the combination of the attributes of a three-dimensional cage scaffold with the distinctive characteristic of boron, thereby offering unusual and versatile pharmacophores in the realm of drug discovery. Numerous research studies have shown that carborane-containing drug molecules proved to be more effective than those of their organic counterparts.[23] On the other hand, N-heterocycles are also widely used in drug molecules, including antitumor drugs in clinical use. Based

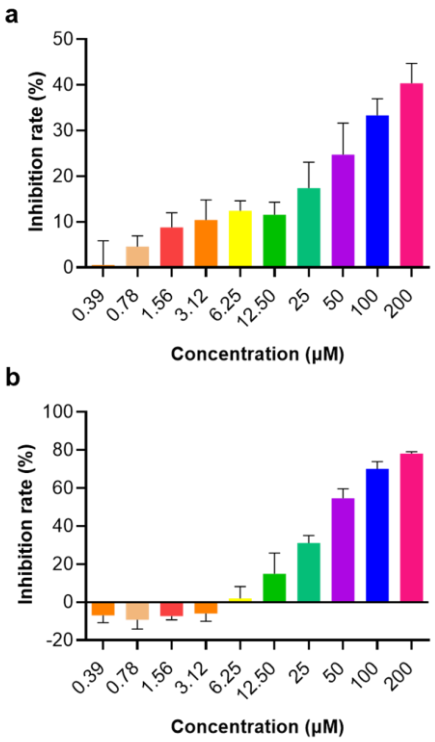

Figure 6. The inhibition rates of compound **8-1** on A431 (**a**) and Hep3B cells (**b**).

on the advantages of both *nido*-carboranes and N-heterocycles, we have developed several *nido*-carborane-based drug candidates (**8-1** to **8-6**) in 80–90% isolated yields through the facile late-stage modification of the commercial drugs such as nikethamide, nicotinyl alcohol, tropicamide, abiraterone acetate, miconazole, and clotrimazole by the current synthetic protocol (Scheme 4a). Compounds **8-1** to **8-4** were further selected for activity tests (Figures 6 and S15). In doing so, we chose cisplatin (DDP), a broad-spectrum antineoplastic drug as the positive comparator, and A431 (epidermal cancer cells) and Hep3B (human hepatoma cells) cells as the target tumor cells. As a result, compound **8-1** showed good antitumor activity on both A431 and Hep3B cells (Figure 6), suggesting that *nido*-carborane-substituted pharmaceutical molecules may have potential for new drug discovery.

Additionally, boron neutron capture therapy (BNCT)[24] is a noninvasive but precise cancer treatment. When ^{10}B-containing molecules/drugs are exposed to thermal neutrons high-energy particles can be generated which are capable of killing cancer cells. Owing to the excellent pharmacological properties of low toxicity and high boron content, boron cluster derivatives hold great potential for the development of new BNCT drugs.[25] Until now, only one clinically used BNCT drug, mercaptoundecahydro-dodecaborate (**BSH**),[24] was developed based on boron cluster. However, **BSH** lacks targeting capability towards cancer cells. Generally, cancer cells need a large quantity of amino acids. Amino acids are also frequently utilized as a pivotal unit for pharmacophores. In this study, two phenylalanine-incorporated *nido*-carborane samples of compounds **8-7** and **8-8** were designed and synthesized by using the developed synthetic methodology (Scheme 4b). Clearly, the current reaction protocol could provide facile access to a molecular library of BNCT drug candidates.

CONCLUSION

We have demonstrated a novel strategy for the straightforward and site-selective B–H functionalization of *nido*-carboranes by facile photoinduced *nido-carborane* cage activation. This protocol is the first example to create the *nido*-carborane cage radical by means of photoinduced boron cage to π charge transfer via a non-covalent cage···π interaction. The resulting *nido*-carborane cage radical initiates subsequent HAT to yield highly reactive *nido*-carborane cage. This approach shows generality, robustness, versatility, and practicality as demonstrated by a wide range of substrates of up to 75 examples, high reaction yields of up to 99%, exclusive regioselectivity at B(9) site of *nido*-carborane cage, and mild reaction conditions (such as an inexpensive photocatalyst of acridinium salt, green light, air as oxidant, room temperature, and short reaction time). By using this protocol, both *nido*-carborane-modified drugs and BNCT drug candidates can be accessed in one step in satisfying yields. Therefore, this study not only enriches the methodologies for the functionalization of *nido*-carboranes but also lays the foundation for the facile synthesis of carborane-based functional molecules.

ASSOCIATED CONTENT

Supporting Information. Experimental details, synthetic procedures, characterization data, crystallographic data, mechanistic studies, and computational details of this article are available free of charge *via* the Internet at pubs.acs.org.

AUTHOR INFORMATION

Corresponding Author

*Hong Yan: hyan1965@nju.edu.cn

*Deshuang Tu: tudeshuang@126.com

*Xingwei Guo: xingwei_guo@mail.tsinghua.edu.cn

*Jordi Poater: jordi.poater@ub.edu

*Miquel Solà: miquel.sola@udg.edu

ACKNOWLEDGMENT

This work is supported by the National Natural Science Foundation of China (92261202 and 21820102004), the Ministry of Science and Technology (2021YFE0114800) and the Natural Science Foundation of Jiangsu Province (BZ2022007), Henan Normal University, the Ministerio de Ciencia e Innovación of Spain (PID2020-113711GB-I00, PID2022-138861NB-I00, PID2019-106830GB-I00, and CEX2021-001202-M), and the Generalitat de Catalunya (2021SGR623 and 2021SGR442). We are grateful to Prof. Shengfa Ye and Mr. Haowei Chen for their helpful discussions on EPR. The Tsinghua University Dushi

Program and the high-performance computing center of Nanjing University are acknowledged. We also appreciate the help from Yunzhi Lin for providing computing time.

REFERENCES

(1) For selected references of the organoboron chemistry, see: (a) Hu, J. F.; Ferger, M.; Shi, Z. Z.; Marder, T. B. Recent Advances in Asymmetric Borylation by Transition Metal Catalysis. *Chem. Soc. Rev.* **2021**, *50*, 13129–13188. (b) Tian, Y. M.; Guo, X. N.; Braunschweig, H.; Radius, U.; Marder, T. B. Photoinduced Borylation for the Synthesis of Organoboron Compounds. *Chem. Rev.* **2021**, *121*, 3561–3597. (c) Peng, T. Y.; Zhang, F. L.; Wang, Y. F. Lewis Base-Boryl Radicals Enabled Borylation Reactions and Selective Activation of Carbon-Heteroatom Bonds. *Acc. Chem. Res.* **2023**, *56*, 169–186. (d) Yang, K.; Song, Q. L. Tetracoordinate Boron Intermediates Enable Unconventional Transformations. *Acc. Chem. Res.* **2021**, *54*, 2298–2312.

(2) (a) Wang, C. L.; Wang, J.; Jin, J. K.; Li, B.; Phang, Y. L.; Zhang, F. L.; Ye, T.; Xia, H. M.; Hui, L. W.; Su, J. H.; Fu, Y.; Wang, Y. F. Boryl Radical Catalysis Enables Asymmetric Radical Cycloisomerization Reactions. *Science* **2023**, *382*, 1056–1065. (b) Lv, J. H.; Chen, A. Y.; Xue, A, S.; Zhao, B. L.; Liang, Y.; Wang, M. Y.; Li, Q.; Yuan, Y.; Han, Y.; Zhao, Y.; Lu, Y.; Zhao, G.; Sun, W. Y.; Houk, K. N.; Shi, Z. Z. Metal-free Directed sp^2–C–H Borylation. *Nature* **2019**, *575*, 336–340. (c) Li, Y. Y.; Li, Y. Q.; Shi, H. J.; Wei, H.; Li, H. Y.; Funes-Ardoiz, I.; Yin, G. Y. Modular Access to Substituted Cyclohexanes with Kinetic Stereocontrol. *Science* **2022**, *376*, 749–753. (d) Jin, S. G.; Liu, K.; Wang, S.; Song, Q. L. Enantioselective Cobalt-Catalyzed Cascade Hydrosilylation and Hydroboration of Alkynes to Access Enantioenriched 1,1-Silylboryl Alkanes. *J. Am. Chem. Soc.* **2021**, *143*, 13124–13134. (e) Zhang, F. Y.; Rauch, F.; Swain, A.; Marder, T. B.; Ravat, P. Efficient Narrowband Circularly Polarized Light Emitters Based on 1,4-B, N-embedded Rigid Donor-Acceptor Helicenes. *Angew. Chem. Int. Ed.* **2023**, *62*, e202218965. (f) Zhao, H. L.; Zhao, C. Y.; Chen, L. L.; Xia, C. G.; Hong, X.; Xu, S. M. Aryl Chloride-Directed Enantioselective C(sp^2)-H Borylation Enabled by Iridium Catalysis. *J. Am. Chem. Soc.* **2023**, *145*, 25214–25221. (g) Yu, Y. J.; Zhang, F. L.; Peng, T. Y.; Wang, C. L.; Cheng, J.; Chen, C.; Houk, K. N.; Wang, Y. F. Sequential C–F Bond Functionalizations of Trifluoroacetamides and Acetates via Spin-center Shifts. *Science* **2021**, *371*, 1232–1240. (h) Zhang, X. L.; Rauch, F.; Niedens, J.; da Silva, R. B.; Friedrich, A.; Nowak-Krol, A.; Garden, S. J.; Marder, T. B. Electrophilic C–H Borylation of Aza[5]helicenes Leading to Bowl-Shaped Quasi-[7]Circulenes with Switchable Dynamics. *J. Am. Chem. Soc.* **2022**, *144*, 22316–22324. (i) Zhao, Q.; Li, B.; Zhou, X.; Wang, Z.; Zhang, F. L.; Li, Y. M.; Zhou, X. G.; Fu, Y.; Wang, Y. F. Boryl Radicals Enabled a Three-Step Sequence to Assemble All-Carbon Quaternary Centers from Activated Trichloromethyl Groups. *J. Am. Chem. Soc.* **2022**, *144*, 15275–15285. (j) Chen, D.; Xu, L. X.; Wang, Z.; Liu, C. Enriched ^{10}B–Diboron Reagents Synthesis from $^{10}BF_3$. *Chem* **2023**, *9*, 3212–3223.

(3) Grimes, R. M. Carboranes. 3rd Ed. *Amsterdam: Academic Press,* **2016**.

(4) (a) Poater, J.; Vinas, C.; Bennour, I.; Gordils, S. E.; Sola, M.; Teixidor, F. Too Persistent to Give Up: Aromaticity in Boron Clusters Survives Radical Structural Changes. *J. Am. Chem. Soc.* **2020**, *142*, 9396–9407. (b) Poater, J.; Viñas, C.; Solà, M.; Teixidor, F. 3D and 2D Aromatic Units Behave Like Oil and Water in the Case of Benzocarborane Derivatives. *Nat. Commun.* **2022**, *13*, 3844.

(5) Hosmane, N. S.; Eagling, R. D. *Handbook of Boron Science: With Applications in Organometallics, Catalysis, Materials and Medicine*; World Scientific: London, **2018**.

(6) For selected references of *closo*-carboranes, see: (a) Mirabelli, M. G. L.; Sneddon, L. G. Transition-Metal-Promoted Reactions of Boron Hydrides. 9.[1] Cp*Ir-Catalyzed Reactions of Polyhedral Boranes and Acetylenes. *J. Am. Chem. Soc.* **1988**, *110*, 449–453. (b) Bregadze, V. I. Dicarba-*closo*-dodecaboranes $C_2B_{10}H_{12}$ and Their Derivatives. *Chem. Rev.* **1992**, *92*, 209–223. (c) Herberhold, M.; Yan, H.; Milius, W.; Wrackmeyer, B. Rhodium-induced Selective B(3)/B(6)-Disubstitution of *ortho*-Carborane-1,2-Dithiolate. *Angew. Chem. Int. Ed.* **1999**, *38*, 3689–3691. (d) Olid, D.; Nunez, R.; Vinas, C.; Teixidor, F. Methods to Produce B–C, B–P, B–N and B–S Bonds in Boron Clusters. *Chem. Soc. Rev.* **2013**, *42*, 3318–3336. (e) Qiu, Z. Z.; Quan, Y. J.; Xie, Z. W. Palladium-Catalyzed Selective Fluorination of *o*-Carboranes. *J. Am. Chem. Soc.* **2013,** *135*, 12192-12195. (f) Lin, F.; Yu, J. L.; Shen, Y.; Zhang, S. Q.; Spingler, B.; Liu, J.; Hong, X.; Duttwyler, S. Palladium-Catalyzed Selective Five-Fold Cascade Arylation of the 12-Vertex Monocarborane Anion by B-H Activation. *J. Am. Chem. Soc.* **2018,** *140*, 13798–13807. (g) Zhang, X. L.; Yan, H. Transition Metal-induced B-H Functionalization of *o*-Carborane. *Coord. Chem. Rev.* **2019**, *378*, 466–482.

(7) For selected references of *closo*-carboranes, see: (a) Qiu, Z. Z.; Xie, Z. W. A Strategy for Selective Catalytic B-H Functionalization of *o*-Carboranes. *Acc. Chem. Res.* **2021**, *54*, 4065–4079. (b) Zhang, X. L.; Zheng, H. M.; Li, J.; Xu, F.; Zhao, J.; Yan, H. Selective Catalytic B-H Arylation of *o*-Carboranyl Aldehydes by a Transient Directing Strategy. *J. Am. Chem. Soc.* **2017**, *139*, 14511–14517. (c) Baek, Y.; Cheong, K.; Ko, G. H.; Han, G. U.; Han, S. H.; Kim, D.; Lee, K.; Lee, P. H. Iridium-catalyzed Cyclative Indenylation and Dienylation through Sequential B(4)–C Bond Formation, Cyclization, and Elimination from *o*-Carboranes and Propargyl Alcohols. *J. Am. Chem. Soc.* **2020**, *142*, 9890–9895. (d) Cao, K.; Xu, T. T.; Wu, J.; Zhang, C. Y.; Wen, X. Y.; Yang, J. The in Situ NHC-palladium Catalyzed Selective Activation of B(3)–H or B(6)–H Bonds of *o*-Carboranes for Hydroboration of Alkynes: An Efficient Approach to Alkenyl-*o*-carboranes. *Inorg. Chem.* **2021**, 60, 1080–1085. (e) Cheng, R. F.; Zhang, J.; Zhang, H. F.; Qiu, Z. Z.; Xie, Z. W. Ir-catalyzed Enantioselective B–H Alkenylation for Asymmetric Synthesis of Chiral-at-Cage-*o*-Carboranes. *Nat. Commun.* **2021**, *12*, 7146. (f) Cao, H. J.; Chen, M.; Sun, F. X.; Zhao, Y.; Lu, C. S.; Zhang, X. L.; Shi, Z. Z.; Yan, H. Variable Metal Chelation Modes and Activation Sequence in Pd Catalyzed B–H Poly-arylation of Carboranes. *ACS. Catal.* **2021**, *11*, 14047–14057. (g) Ma, Y. N.; Gao, Y.; Ma, Y. B.; Wang, Y.; Ren, H. Z.; Chen, X. N. Palladium-Catalyzed Regioselective B(9)-Amination of *o*-Carboranes and *m*-Carboranes in HFIP with Broad Nitrogen Sources. *J. Am. Chem. Soc.* **2022**, *144*, 8371–8378.

(8) For selected references of *closo*-carboranes, see: (a) Zhao, D.; Xie, Z. W. Visible-Light-Promoted Photocatalytic B–C Coupling via a Boron-Centered Carboranyl Radical: Facile Synthesis of B(3)-Arylated *o*-Carboranes. *Angew. Chem. Int. Ed.* **2016**, 55, 3166–3170. (b) Mills, H. A.; Martin, J. L.; Rheingold, A. L.; Spokoyny, A. M. Oxidative Generation of Boron-Centered Radicals in Carboranes. *J. Am. Chem. Soc.* **2020**, *142*, 4586–4591. (c) Chen, M.; Xu, J. K.; Zhao, D. S.; Sun, F. X.; Tian, S. L.; Tu, D. S.; Lu, C. S.; Yan, H. Site-Selective Functionalization of Carboranes at the Electron-Rich Boron Vertex: Photocatalytic B-C Coupling via a Carboranyl Cage Radical. *Angew. Chem. Int. Ed.* **2022**, *61*, e202205672. (d) Hamdaoui, M.; Liu, F.; Cornaton, Y.; Lu, X. Y.; Shi, X. H.; Zhang, H.; Liu, J. Y.; Spingler, B.; Djukic, J. P.; Duttwyler, S. An Iridium-Stabilized Borenium Intermediate. *J. Am. Chem. Soc.* **2022**, *144*, 18359–18374. (e) Cui, P. F.; Liu, X. R.; Jin, G. X. Supramolecular Architectures Bearing Half-Sandwich Iridium- or Rhodium-Based Carboranes: Design, Synthesis, and Applications. *J. Am. Chem. Soc.* **2023**, *145*, 19440–19457. (f) Ma, Y. N.; Ren, H. Z.; Wu, Y. X.; Li, N.; Chen, F. J.; Chen, X. N. B(9)-OH-*o*-Carboranes: Synthesis, Mechanism, and Property Exploration. *J. Am. Chem. Soc.* **2023,** *145*, 7331–7342.

(9) For selected references of nucleophilic substitution on *nido*-carboranes, see: (a) Tutusaus, O.; Teixidor, F.; Nuńez, R.; Viñas, C.; Sillanpää, R.; Kivekäs, R. Recent Studies on RR'S·$C_2B_9H_{11}$

Charge-compensated Ligands: Crystal Structures of 10-($S(CH_3)_2$)-7,8-$C_2B_9H_{11}$ and 10-($S(CH_2)_4$)-7,8-$C_2B_9H_{11}$. *J. Organomet. Chem.* **2002**, *657*, 247–255. (b) Šícha, V.; Plesek, J.; Kvícalová, M.; Císarová, I.; Grüner, B. Boron (8) Substituted Nitrilium and Ammonium Derivatives, Versatile Cobalt Bis(1,2-Dicarbollide) Building Blocks for Synthetic Purposes. *Dalton Trans.* **2009**, 851–860. (c) Frank, R.; Adhikari, A. K.; Auer, H.; Hey-Hawkins, E. Electrophile-Induced Nucleophilic Substitution of the *nido*-Dicar-Baundecaborate Anion *nido*-7,8-$C_2B_9H_{12}^-$ by Conjugated Heterodienes. *Chem. Eur. J.* **2014**, *20*, 1440–1446. (d) Stogniy, M. Y.; Erokhina, S. A.; Suponitsky, K. Y.; Anisimov, A. A.; Sivaev, I. B.; Bregadze, V. I. Nucleophilic Addition Reactions to the Ethylnitrilium Derivative of *nido*-Carborane 10-EtC≡N-7,8-C2B9H11. *New J. Chem.* **2018,** *42*, 17958–17967. (e) Vinogradov, M. M.; Nelyubina, Y. V.; Aliyeu, T. M. New Aspects of Acid-assisted Nucleophilic Substitution Reactions of 11-Vertex *nido*-Carboranes. *Polyhedron* **2022**, *214*, 115654. (f) Stogniy, M. Y.; Anufriev S. A.; Sivaev, I. B. Charge-Compensated Derivatives of *nido*-Carborane. *Inorganics* **2023**, *11*, 72.

(10) For selected references of electrophilic substitution on *nido*-carboranes, see: (a) Olsen, F. P.; Hawthorne, M. F. Synthesis and Structural Characterization of $[(CH_3)_3NH][nido\text{-}9,11\text{-}I_2\text{-}7,8\text{-}C_2B_9H_{10}]$ and $[(CH_3)_3NH][nido\text{-}9\text{-}I\text{-}7,8\text{-}C_2B_9H_{11}]$. *Inorg. Chem.* **1965**, *4*, 1839–1840. (b) Mizusawa, E. A.; Thompson, M. R.; Hawthorne, M. F. Synthesis and Antibody-Labeling Studies with the *p*-Isothiocyanatobenzene Derivatives of 1,2-Dicarba-*closo*-Dodecarborane(12) and the Dodecahydro-7,8-Dicarbanido-Undecaborate(-1) Ion for Neutron-Capture Therapy of Human Cancer. Crystal and Molecular Structure of $Cs^+[nido\text{-}7\text{-}(p\text{-}C_6H_4NCS)\text{-}9\text{-}I\text{-}7,8\text{-}C_2B_9H_{11}]^-$. *Inorg. Chem.* **1985**, *24*. 1911–1916. (c) Santos, E. C.; Pinkerton, A. B.; Kinkead, S. A.; Hurlburt, P. K.; Jasper, S. A.; Sellers, C. W.; Huffman, J. C.; Todd, L. J. Syntheses of *nido*-9,11-X_2-7,8-$C_2B_9H_{10}^-$ Anions (X=Cl, Br or I) and the Synthesis and Structural Characterization of $N(C_2H_5)_4[commo\text{-}3,3'\text{-}Co(4,7\text{-}Br_2\text{-}3,1,2\text{-}CoC_2B_9H_9)_2]$. *Polyhedron* **2000**, *19*, 1777–1781. (d) Rudakov, D. A.; Shirokii, V. L.; Potkin, V. I.; Dikusar, E. A.; Bragin, V. I.; Petrovskii, P. V.; Sivaev, I. B.; Bregadze, V. I.; Kisin, A. V. Electrochemical Iodination of C-methyl Derivatives of Dodecahydro-7,8-Dicarba-*nido*-Undecaborate Anion. *Russ. J. Electrochem.* **2006**, *42*, 280–284. (e) Frank, F.; Grell, T.; Hiller, M.; Hey-Hawkins, E. Electrophilic Substitution of *nido*-Dicarbaborate Anion 7,8-*nido*-$C_2B_9H_{12}^-$ with Sulfenyl Chlorides. *Dalton Trans.* **2012**, *41*, 6155–6161.

(11) For selected references of oxidative substitution on *nido*-carboranes, see: (a) Zakharkin, L. I.; Kalinin, V. N.; Zhigareva, G. G. Oxidation of Dicarbadodecahydronidoundecaborate Anions by Mercuric Chloride in Tetrahydrofuran and Pyridine. *Russ. Chem. Bull.* **1979**, *28*, 2198–2199. (b) Kang, H. C.; Lee, S. S.; Knobler, C. B.; Hawthorne, M. F. Syntheses of Charge-compensated Dicarbollide Ligand Precursors and their Use in the Preparation of Novel Metallacarboranes. *Inorg. Chem.* **1991**, *30*, 2024–2031. (c) Stogniy, M. Y.; Abramova, E. N.; Lobanova, I. A.; Sivaev, I. B.; Bragin, V. I.; Petrovskii, P. V.; Tsupreva, V. N.; Sorokina, O. V.; Bregadze, V. I. Synthesis of Functional Derivatives of 7,8-Dicarba-*nido*-Undecaborate Anion by Ring-Opening of its Cyclic Oxonium Derivatives. *Collect. Czech. Chem. Commun.* **2007**, *72*, 1676–1688. (d) Grüner, B.; Holub, J.; Plesek, J.; Š tíbr, B.; Thornton-Pett, M.; Kennedy, J. D. Dimethylsulfide-Dicarbaborane Chemistry. Isolation and Characterization of Isomers [9-(SMe_2)-*nido*-7,8-$C_2B_9H_{10}$-X-Me] (where X = 1, 2, 3 and 4) and Some Related Compounds. An Unusual Skeletal Rearrangement. *Dalton Trans.* **2007**, 4859–4865. (e) Yang, L.; Jei, B. B.; Scheremetjew, A.; Kuniyil, R.; Ackermann, L. Electrochemical B–H Nitrogenation: Access to Amino Acid and BODIPY-Labeled *nido*-Carboranes. *Angew. Chem. Int. Ed.* **2021**, *60*, 1482–1487. (f) Chen, M.; Zhao, D.; Xu, J.; Li, C.; Lu, C.; Yan, H. Electrooxidative B–H Functionalization of *nido*-Carboranes. *Angew. Chem. Int. Ed.* **2021**, *60*, 7838–7844.

(12) For selected references of metal mediation for *nido*-carboranes, see: (a) Hewes, J. D.; Kreimendahl, C. W.; Marder, T. B.; Hawthorne, M. F. Metal-Promoted Insertion of an Activated Alkene into a B–H Bond of an Exopolyhedra *nido*-Rhodacarboran-Rhodium-Catalyzed Hydroboration. *J. Am. Chem. Soc.* **1984**, *106*, 5757–5759. (b) Jasper, S. A.; Mattern, J.; Huffman, J. C.; Todd, L. J. Palladium-Mediated Substitution of the *closo*-$B_{12}H_{12}(-2)$ and *nido*-7,8-$C_2B_9H_{12}(-1)$ Ions by PMe2Ph: The Single-crystal Structure Studies of 1,7-$(PMe_2Ph)_2$-*closo*-$B_{12}H_{10}$ and 9-PMe_2Ph-*nido*-7,8-$C_2B_9H_{11}$. *Polyhedron* **2007,** *26*, 3793–3798. (c) Timofeev, S. V.; Zhidkova, O. B.; Prikaznova, E. A.; Sivaev, I. B.; Semioshkin, A.; Godovikov, I. A.; Starikova, Z. A.; Bregadze, V. I. Direct Synthesis of *nido*-Carborane Derivatives with Pendant Functional Groups by Copper-Promoted Reactions with Dimethylalkylamines. *J. Organomet. Chem.* **2014,** *757*, 21–27. (d) Sun, F. X.; Tan, S. M.; Cao, H. J.; Xu, J. K.; Bregadze, V. I.; Tu, D. S.; Lu, C. S.; Yan, H. Palladium-Catalyzed Hydroboration of Alkynes with Carboranes: Facile Construction of a Library of Boron Cluster-Based AIE-Active Luminogens. *Angew. Chem. Int. Ed.* **2022**, *61*, e202207125. (e) Sun, C.; Lu, J. Y.; Lu, J. Pd-Catalyzed Selective B(6)–H Phosphorization of *nido*-Carboranes via Cascade Deboronation/B–H Activation from *closo*-Carboranes. *Inorg. Chem.* **2022**, *61*, 9623–9630. (f) Sun, F. X.; Tan, S. M.; Cao, H. J.; Lu, C. S.; Tu, D. S.; Poater, J.; Sola, M.; Yan, H. Facile Construction of New Hybrid Conjugation via Boron Cage Extension. *J. Am. Chem. Soc.* **2023**, *145*, 3577–3587.

(13) Yu, J. Q.; Shi, Z. J. *C–H Activation.* Springer: Berlin, Heidelberg, **2010**, 380.

(14) Tu, D. S.; Yan, H.; Poater, J.; Sola, M. The *nido*-cage···π Bond: A Non-Covalent Interaction between Boron Clusters and Aromatic Rings and Its Applications. *Angew. Chem. Int. Ed.* **2020**, *59*, 9018–9025.

(15) For selected references on EDA complexes involved photocatalysis, see: (a) Fu, M. C.; Shang, R.; Zhao, B.; Wang, B.; Fu, Y. Photocatalytic Decarboxylative Alkylations Mediated by Triphenylphosphine and Sodium Iodide. *Science* **2019**, *363*, 1429–1434. (b) Arceo, E.; Jurberg, I. D.; Álvarez-Fernández, A.; Melchiorre, P. Photochemical Activity of a Key Donor-acceptor Complex Can Drive Stereoselective Catalytic α-Alkylation of Aldehydes. *Nat. Chem.* **2013**, 5, 750–756. (c) Crisenza, G. E. M.; Mazzarella, D.; Melchiorre, P. Synthetic Methods Driven by the Photoactivity of Electron Donor-Acceptor Complexes. *J. Am. Chem. Soc.* **2020**, *142*, 5461–5476. (d) Dewanji, A.; Van Dalsen, L.; Rossi-Ashton, J. A.; Gasson, E.; Crisenza, G. E. M.; Procter, D. J. A General Arene C–H Functionalization Strategy via Electron Donor-acceptor Complex Photoactivation. *Nat. Chem.* **2023**, *15*, 43–52.

(16) For selected references of the photocatalyst acridinium, see: (a) Fukuzumi, S.; Ohkubo, K.; Suenobu, T.; Kato, K.; Fujitsuka, M.; Ito, O. Photoalkylation of 10-Alkylacridinium Ion via a Charge-shift Type of Photoinduced Electron Transfer Controlled by Solvent Polarity. *J. Am. Chem. Soc.* **2001,** *123*, 8459–8467. (b) Margrey, K. A.; Nicewicz, D. A. A General Approach to Catalytic Alkene Anti-Markovnikov Hydrofunctionalization Reactions via Acridinium Photoredox Catalysis. *Acc. Chem. Res.* **2016**, *49*, 1997–2006. (c) Pramanik, M.; Choudhuri, K.; Mathur, A.; Mal, P. Dithioacetalization or Thioetherification of Benzyl Alcohols Using 9-Mesityl-10-Methylacridinium Perchlorate Photocatalyst. *Chem. Commun.* **2020**, *56*, 10211–10214. (d) Hoshino, M.; Uekusa, H.; Tomita, A.; Koshihara, S. Y.; Sato, T.; Nozawa, S.; Adachi, S.; Ohkubo, K.; Kotani, H.; Fukuzumi, S. Determination of the Structural Features of a Long-lived Electron-transfer State of 9-mesityl-10-methylacridinium Ion. *J. Am. Chem. Soc.* **2012**, *134*, 4569–72. (e) Wan, T.; Capaldo, L.; Ravelli, D.; Vitullo, W.; Zwart, F. J.; Bruin, B.; Noel, T. Photoinduced Halogen-Atom Transfer by N-Heterocyclic Carbene-Ligated Boryl Radicals for C(sp^3)-C(sp^3) Bond Formation. *J. Am. Chem. Soc.* **2023**, *145*, 991–999.

(17) For selected references of the photoredox catalysis, see: (a) Hu, A. H.; Guo, J. J.; Pan, H.; Zuo, Z. W. Selective Functionalization of Methane, Ethane, and Higher Alkanes by Cerium Photocatalysis. *Science* **2018**, *361*, 668–672. (b) Chan, A. Y.; Perry, I. B.; Bissonnette, N. B.; Buksh, B. F.; Edwards, G. A.; Frye, L. I.; Garry, O. L.; Lavagnino, M. N.; Li, B. X.; Liang, Y.; Mao, E.; Millet, A.; Oakley, J. V.; Reed, N. L.; Sakai, H. A.; Seath, C. P.; MacMillan, D. W. C. Metallaphotoredox: The Merger of Photoredox and Transition Metal Catalysis. *Chem. Rev.* **2022**, *122*, 1485–1542. (c) Holmberg-Douglas, N.; Nicewicz, D. A. Photoredox-Catalyzed C–H Functionalization Reactions. *Chem. Rev.* **2022**, *122*, 1925–2016. (d) Lu, F. D.; Chen, J.; Jiang, X.; Chen, J. R.; Lu, L. Q.; Xiao, W. J. Recent Advances in Transition-Metal-Catalysed Asymmetric Coupling Reactions with Light Intervention. *Chem. Soc. Rev.* **2021**, *50*, 12808–12827. (e) Wen, L.; Ding, J.; Duan, L. F.; Wang, S.; An, Q.; Wang, H. X.; Zuo, Z. W. Multiplicative Enhancement of Stereoenrichment by a Single Catalyst for Deracemization of Alcohols. *Science* **2023**, *382*, 459–464.

(18) Ren, H. Y.; Zhang, P.; Xu, J. K.; Ma, W. L.; Tu, D. S.; Lu, C. S.; Yan, H. Direct B–H Functionalization of Icosahedral Carboranes via Hydrogen Atom Transfer. *J. Am. Chem. Soc.* **2023**, *145*, 7638–7647.

(19) Zhang, S. X.; Zhou, S. Q.; Qi, J. Q.; Jiao, L.; Guo, X. W. Time-resolved Electron Paramagnetic Resonance Spectrometer Based on Ultrawide Single-sideband Phasesensitive Detection. *Rev. Sci. Instrum.* **2023**, *94*, 084101. (b) Qi, J. Q.; Suo, W. Q.; Liu, J.; Sun, S. T.; Jiao, L.; Guo, X. W. Watching a Full Photocatalytic Cycle by Electron Paramagnetic Resonance. DOI: 10.26434/chemrxiv-2023-tbw7q.

(20) For selected references of EPR for the boron clusters, see: (a) Kaim, W.; Hosmane, N. S.; Zalis, S.; Maguire, J. A.; Lipscomb, W. N. Boron Atoms as Spin Carriers in Two- and Three-Dimensional Systems. *Angew. Chem. Int. Ed.* **2009**, *48*, 5082–5091. (b) Stauber, J. M.; Schwan, J.; Zhang, X.; Axtell, J. C.; Jung, D.; McNicholas, B. J.; Oyala, P. H.; Martinolich, A. J.; Winkler, J. R.; See, K. A.; Miller, T. F.; Gray, H. B.; Spokoyny, A. M. A Super-Oxidized Radical Cationic Icosahedral Boron Cluster. *J. Am. Chem. Soc.* **2020**, *142*, 12948–12953.

(21) Yang, Z. M.; Zhao, W. J.; Liu, W.; Wei, X.; Chen, M.; Zhang, X.; Zhang, X. L.; Liang, Y.; Lu, C. S.; Yan, H. Metal-Free Oxidative B–N Coupling of *nido*-Carborane with N–Heterocycles. *Angew. Chem. Int. Ed.* **2019**, *58*, 11886–11892.

(22) Cigler, P.; Kozisek, M.; Rezacova, P.; Brynda, J.; Otwinowski, Z.; Pokorna, J.; Plesek, J.; Gruner, B.; Doleckova-Maresova, L.; Masa, M.; Sedlacek, J.; Bodem, J.; Krausslich, H.; Kra, V.; Konvalinka, J. From Nonpeptide toward Noncarbon Protease Inhibitors: Metallacarboranes as Specific Andpotent Inhibitors of HIV Protease. *PNAS* **2005**, *102*, 15394–15399.

(23) For selected references of the carborane derivatives for drug candidates, see: (a) Stockmann, P.; Gozzi, M.; Kuhnert, R.; Sarosi, M. B.; Hey-Hawkins, E. New Keys for Old Locks: Carborane-containing Drugs as Platforms for Mechanism-based Therapies. *Chem. Soc. Rev.* **2019**, *48*, 3497–3512. (b) Issa, F.; Kassiou, M.; Rendina, L. M. Boron in Drug Discovery: Carboranes as Unique Pharmacophores in Biologically Active Compounds. *Chem. Rev.* **2011**, *111*, 5701–5722.

(24) Hosmane, N. S.; Maguire, J. A.; Zhu, Y.; Takagaki, M. Future Perspectives for Boron and Gadolinium Neutron Capture Therapies in Cancer Treatment. *In Boron and Gadolinium Neutron Capture Therapy for Cancer Treatment*. World Scientific: Singapore, Chapter 9, **2011**, 165–170.

(25) For selected references of the BNCT drug candidates, see: (a) Salt, C.; Lennox, A. J.; Takagaki, M.; Maguire, J. A.; Hosmane, N. S. Boron and Gadolinium Neutron Capture Therapy. *Russ. Chem. Bull. Int. Ed.* **2004**, *53*, 1871–1888. (b) Zhu, Y. H.; Peng, A. T.; Carpenter, K.; Maguire, J. A.; Hosmane, N. S.; Takagaki, M. Substituted Carborane-Appended Water-Soluble Single-Wall Carbon Nanotubes: New Approach to Boron Neutron Capture Therapy Drug Delivery. *J. Am. Chem. Soc.* **2005**, *127*, 9875–9880. (c) Hey-Hawkins, E.; Teixidor, C. V. Boron-Based Compounds: Potential and Emerging Applications in Medicine. *John Wiley & Sons Ltd,* Chapter 1.1, **2018**, 1–19. (d) Li, J. Y.; Sun, Q.; Lu, C. J.; Xiao, H.; Guo, Z. B.; Duan, D. B.; Zhang, Z. Z.; Liu, T.; Liu, Z. B. Boron Encapsulated in a Liposome Can be Used for Combinational Neutron Capture Therapy. *Nat. Commun.* **2022,** *13*, 2143.

Insert Table of Contents artwork here